Modeling and Simulation of Joint Time-Frequency Properties of Spectrum Usage in Cognitive Radio

Invited Paper

Miguel López-Benítez, Fernando Casadevall
Dept. of Signal Theory and Communications
Universitat Politècnica de Catalunya (UPC)

David López-Pérez
Centre for Telecommunications Research
King's College London

Athanasios V. Vasilakos
Dept. of Computer and Telecommunications Engineering
University of Western Macedonia

ABSTRACT

The development of the Dynamic Spectrum Access/Cognitive Radio (DSA/CR) technology can significantly benefit from the availability of realistic models able to accurately capture and reproduce the statistical properties of spectrum usage in real wireless communication systems. Relying on field measurements of real systems, this paper analyzes the joint time-frequency statistical properties of spectrum usage and develops adequate models describing the observed characteristics. Based on such models, a sophisticated method is also proposed to generate artificial spectrum data for simulation or other purposes. The proposed method is able to accurately reproduce the statistical time-frequency characteristics of spectrum usage in real systems.

Categories and Subject Descriptors

I.6 [**Simulation and modeling**]: Model development—*modeling methodologies*; I.6 [**Simulation and modeling**]: Model validation and analysis

General Terms

Algorithms

Keywords

cognitive radio, dynamic spectrum access, spectrum characterization, spectrum occupancy modeling

1. INTRODUCTION

Most of spectrum with commercially attractive radio propagation characteristics has already been allocated in many countries, a situation commonly referred to as *spectrum scarcity problem*. Various spectrum measurement campaigns [8] have demonstrated, however, that spectrum is vastly underutilized and the virtual scarcity actually results from inefficient spectrum access policies. This situation has motivated the emergence of Dynamic Spectrum Access (DSA) policies based on the Cognitive Radio (CR) paradigm [1]. The basic underlying principle of DSA/CR is to allow unlicensed users to access in an opportunistic and non-interfering manner some licensed bands temporarily unoccupied by the licensed users. Unlicensed (secondary) DSA/CR terminals sense the spectrum in order to detect spectrum gaps left by licensed (primary) users and transmit on them. Secondary unlicensed transmissions are allowed following this operating principle as long as they do not induce harmful interference levels on the primary network.

As a result of the opportunistic nature of the DSA/CR paradigm, the behavior and subsequent performance of a DSA/CR network is tightly related to the spectrum occupancy patterns of the primary networks. The development of realistic and accurate models capable to describe such patterns would therefore be significantly useful in the domain of DSA/CR research. Spectrum usage models can find many fields of application ranging from analytical studies to the design and dimensioning of DSA/CR networks, including the development of innovative simulation tools as well as novel DSA/CR techniques. The usefulness of spectrum models is however conditioned on their realism and accuracy. Models for spectrum usage commonly employed to date in DSA/CR research are limited in scope and based on oversimplifications or assumptions that have not been validated with empirical measurement data. Spectrum modeling in DSA/CR still constitutes a rather unexplored research area.

In this context, this paper addresses the problem of jointly modeling spectrum occupancy in the time and frequency domains. Previous work [5, 6] has dealt with the question of modeling and reproducing spectrum occupancy patterns of individual channels and their properties in the time domain. This work extends previous studies by including the frequency dimension. The objective is to develop adequate models capable to capture and reproduce the time evolution of the occupancy patterns observed in a group of channels belonging to the same allocated spectrum band. This is an important aspect since it has a direct impact on the amount of consecutive vacant spectrum that a DSA/CR user may find as well as the time period for which spectrum gaps can be exploited for opportunistic use. This paper analyzes the statistical time-frequency characteristics of spectrum usage based on empirical data from an extensive spectrum measurement campaign. Based on the obtained results, adequate models are proposed. Moreover, a sophisticated procedure is developed in order to generate artificial spectrum occupancy data, for simulation or other purposes, capable to reproduce the statistical time-frequency characteristics of spectrum usage in real systems.

CogART'11, October 26 - 29 2011, Barcelona, Spain

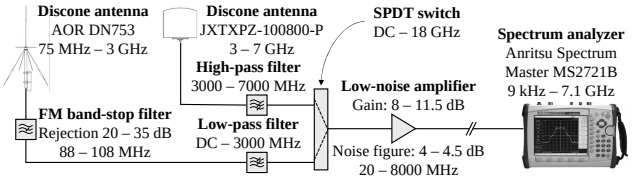

Figure 1: Employed measurement setup.

2. MEASUREMENT SETUP

The measurement configuration employed in this work (see Figure 1) relies on a spectrum analyzer setup where different external devices have been added in order to improve the detection capabilities. The design is composed of two broadband discone-type antennas covering the frequency range from 75 to 7075 MHz, a Single-Pole Double-Throw (SPDT) switch to select the desired antenna, several filters to remove undesired overloading (FM) and out-of-band signals, a low-noise pre-amplifier to enhance the overall sensitivity and thus the ability to detect weak signals, and a high performance spectrum analyzer to record the spectral activity. The external amplifier shown in Figure 1 along with the spectrum analyzer's internal amplifier (≈25 dB gain) result in an overall sensitivity around –130 dBm per 10-kHz resolution-bandwidth (4-dB noise figure), which guarantees a reliable estimation of spectrum usage. An exhaustive description of the measurement platform and methodological procedures can be found in [7, 4].

The measurement equipment of Figure 1 was employed to monitor the activity of several spectrum bands including amateur bands (144–146 MHz), paging bands (157–174 MHz), TETRA uplink (410–420 MHz) and downlink (420–430 MHz), E-GSM 900 uplink (880–915 MHz) and downlink (925–960 MHz), DCS 1800 uplink (1710–1785 MHz) and downlink (1805–1880 MHz), DECT (1880–1900 MHz) and ISM (2400–2500 MHz). Although this paper does not present results for all the analyzed spectrum bands, the proposed models were developed and validated based on channels from all the considered radio technologies. Each band was measured for a total time period of 7 days, from Monday midnight to Sunday midnight. The captured data were used to extract the binary occupancy patterns of each individual channel by classifying power samples as either busy or idle states based on an energy detection method [10]. The decision threshold was selected as the maximum noise power observed in each channel (based on measurements of the receiver's noise) plus a 3-dB margin. This criterion was explicitly selected in order to avoid any potential false alarms. The detection performance loss resulting from this relatively high decision threshold was verified to be negligible since the measurement location for each analyzed band was carefully selected in order to maximize the receiving SNR, which guarantees that the probability of missed detections is minimized, thus resulting in a nearly ideal detection performance under such conditions. The resulting occupancy sequences for channels belonging to the same band were compared to analyze the joint time-frequency properties of spectrum.

3. SYSTEM MODEL

The considered system model assumes that the DSA/CR network operates over a set of C radio channels, denoted as $\Upsilon = \{\upsilon_1, \upsilon_2, \ldots, \upsilon_c, \ldots, \upsilon_C\}$. Let's denote as $\mathbb{S} = \{s_0, s_1\}$ the state space for a primary radio channel, where s_0 indicates that the channel is idle and s_1 that the channel is busy. The state of the C channels is simultaneously observed at discrete time instants $t = t_k = kT_s$, where k is a non-negative integer and T_s is the time period elapsed between two consecutive observations. Assuming that the set of channels Υ is observed for K time periods T_s, each channel is characterized by a binary occupancy sequence $\{S_c(t_1), S_c(t_2), \ldots, S_c(t_k), \ldots, S_c(t_K)\}$, where $S_c(t_k)$ denotes the state (s_0 or s_1) of channel υ_c at time instant t_k.

4. TIME-FREQUENCY PROPERTIES

The captured data were extensively analyzed in order to determine whether the binary time-occupancy pattern of a radio channel is related with those of other channels within the same band. The obtained results indicated that the occupancy patterns of individual channels can be considered to be mutually independent. Such independence can be demonstrated based on the fact that two events A and B are independent if and only if their joint probability $P(A, B)$ equals the product of their individual probabilities $P(A)$ and $P(B)$, i.e., $P(A, B) = P(A) \cdot P(B)$. Based on this simple result from the basic theory of probability, the independence between the occupancy patterns of a pair of channels can be determined as follows. First, compute the elements of matrix $\mathbf{P} = [p_{ij}]_{C\times C}$, where $p_{ij} = P(S_i(t_k) = s_1, S_j(t_k) = s_1)$ represents the joint probability that channels υ_i and υ_j are simultaneously observed as busy at any time instant t_k. Then, compute the elements of matrix $\mathbf{Q} = [q_{ij}]_{C\times C}$, where:

$$q_{ij} = \begin{cases} \Psi_i \cdot \Psi_j, & i \neq j \\ \Psi_i = \Psi_j, & i = j \end{cases} \quad (1)$$

where Ψ_i and Ψ_j are the Duty Cycle (DC) of channels υ_i and υ_j, respectively (i.e., the fraction of time they are busy). Finally, compute the difference between both matrices. If $\mathbf{P} - \mathbf{Q} = \mathbf{0}_{C\times C}$, where $\mathbf{0}_{C\times C}$ denotes a $C \times C$ square matrix whose elements are all zero, then the channel occupancy patterns are mutually independent. However, if an appreciable number of elements is non-zero, then this would imply that independence is not a completely realistic assumption.

The proposed procedure is justified as follows. The elements of $\mathbf{P}$ can be expressed as $p_{ij} = P(S_i(t_k) = s_1 \,|\, S_j(t_k) = s_1) \cdot P(S_j(t_k) = s_1)$. If the occupancy patterns of channels υ_i and υ_j are independent, then it must be true that $P(S_i(t_k) = s_1 \,|\, S_j(t_k) = s_1) = P(S_i(t_k) = s_1)$ and in such a case $p_{ij} = P(S_i(t_k) = s_1) \cdot P(S_j(t_k) = s_1)$. Notice that the terms of the last equality represent the probability that the channels are observed as busy or in other words their DCs, i.e., $P(S_i(t_k) = s_1) = \Psi_i$ and $P(S_j(t_k) = s_1) = \Psi_j$. Therefore, if the occupancy patterns of channels υ_i and υ_j are independent, it holds that $p_{ij} = q_{ij}$ and therefore $p_{ij} - q_{ij} = 0$. Notice, however, that this is only true for $i \neq j$ since the elements of the main diagonal of $\mathbf{P}$ are given by $p_{ii} = P(S_i(t_k) = s_1, S_i(t_k) = s_1) = P(S_i(t_k) = s_1) = \Psi_i$, which requires a particular definition of q_{ij} in Equation 1 for $i = j$ in order to guarantee that the equality $\mathbf{P} - \mathbf{Q} = \mathbf{0}_{C\times C}$ holds for all elements in case of independence.

Matrices $\mathbf{P}$ and $\mathbf{Q}$ were estimated based on field measurements. The elements of $\mathbf{P}$ were computed as the number of observations with busy states in each pair of channels divided by the total number K of observations. The elements of $\mathbf{Q}$ were derived based on the empirical DCs of each individual channel, obtained as the quotient between the number of observations with busy state and the total number K of observations. The difference between both matrices was computed for various spectrum bands. Figure 2 shows, as an example, the results obtained for the TETRA DL band, where the absolute values of the elements of the resulting difference matrix are plotted as a function of the channel indexes i and j. This figure is also representative of the results obtained for the rest of bands. As it can be appreciated, the difference matrix is composed of zeros for all channel pairs except for some particular cases whose values are very close to zero. As a result, and based on Figure 2, it

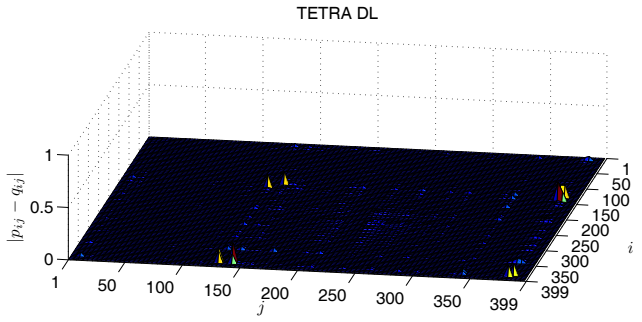

Figure 2: Elements of $\mathrm{abs}\,(\mathbf{P} - \mathbf{Q})$ for TETRA DL.

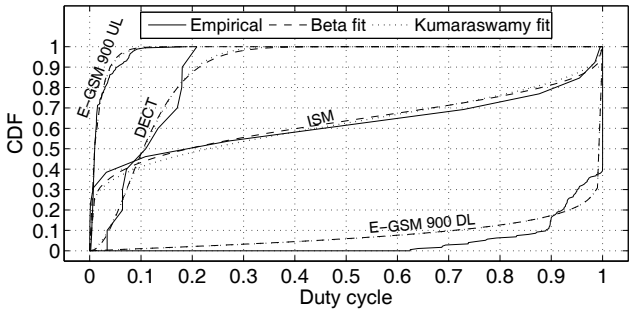

Figure 3: Empirical DC distributions.

can be concluded that the occupancy patterns for channels within a spectrum band can be considered to be mutually independent. This is a result with important implications for joint time-frequency modeling, since it implies that the instantaneous occupancy state of a channel is unrelated to the instantaneous state of the rest of channels within the considered band and, consequently, the occupancy patterns of a group of channels can be modeled independently of each other. On the one hand, this enables the direct application of time-domain models such as those developed in [5, 6] without any modifications or additional considerations. On the other hand, this enables the statistical properties of spectrum usage over frequency to be analyzed independently of the time-dimension statistics.

5. FREQUENCY CHARACTERISTICS

Extensive analyses of measurement data revealed the existence of two aspects deserving explicit consideration, namely the probability distribution of DC values for channels within the same band and the DC clustering over frequency, i.e., the existence of groups of contiguous channels with similar DCs.

5.1 Duty cycle distribution

Given the set $\mathbf{\Psi} = \{\Psi_1, \Psi_2, \ldots, \Psi_c, \ldots, \Psi_C\}$, where Ψ_c represents the DC of channel υ_c, the distribution function of the elements of $\mathbf{\Psi}$ was computed for all the analyzed bands and compared to various models. It was found that the empirical DC distributions can accurately be fitted with beta [9] and Kumaraswamy [3] distributions. The beta distribution can be found in many popular software simulation packages. However, it may present some difficulties in analytical studies due to the complex expression of its density (PDF) and distribution (CDF) functions. The Kumaraswamy distribution is similar to the beta distribution but easier to use in analytical studies due to its simpler form [2]. While the former may be more appropriate for simulations, the latter may be more convenient for analytical studies.

Figure 3 shows some examples of empirical DC distributions and their corresponding beta and Kumaraswamy fits. The selected bands represent examples for very low (E-GSM 900 UL), low (DECT), medium (ISM) and very high (E-GSM 900 DL) average band DCs. As it can be appreciated, the beta and Kumaraswamy distributions are able to provide reasonably accurate fits in all cases. To facilitate the application of these models, Table 1 provides reference values for the distribution parameters, extracted from empirical data by means of maximum likelihood estimation techniques, along with the average band DCs $\overline{\Psi} = (1/C)\sum_{c=1}^{C} \Psi_c$.

5.2 Duty cycle clustering

The analysis of empirical measurement data indicated that channels with similar load levels rarely occur alone, but in

Table 1: Fitted values for DC distributions.

Measured band	Average DC $\overline{\Psi}$	Beta		Kumaraswamy	
		α	β	a	b
Amateur	0.17	0.5796	2.8963	0.6311	2.5599
Paging	0.28	1.4867	3.9601	1.3449	4.2382
TETRA UL	0.03	0.7105	44.0554	0.7849	26.9302
TETRA DL	0.36	0.1840	0.2837	0.1389	0.4223
GSM 900 UL	0.02	1.6044	116.6408	1.2690	208.5805
GSM 900 DL	0.96	0.9119	0.0778	0.8970	0.0786
DCS 1800 UL	0.02	0.2023	6.0738	0.2545	2.6118
DCS 1800 DL	0.44	0.4525	0.6118	0.4463	0.6846
DECT	0.12	2.3217	17.5170	1.7434	34.2432
ISM	0.42	0.2022	0.3418	0.1426	0.4155

groups (clusters) of certain size. To analyze and characterize the DC clustering over frequency, a set of five DC archetypes was defined, namely very low $\Psi \in [0, 0.05]$, low $\Psi \in (0.05, 0.40]$, medium $\Psi \in (0.40, 0.60]$, high $\Psi \in (0.60, 0.95]$ and very high $\Psi \in (0.95, 1]$ levels. The DCs observed in the analyzed spectrum bands were computed and classified into the aforementioned archetypes. Figure 4 shows an example for the TETRA DL band. The upper graph shows the instantaneous spectrum occupancy for each channel for a time period of 60 minutes (white/black points indicate idle/busy observations, respectively), while the lower graph shows the channel DCs (each archetype is represented by a different color). As it can clearly be appreciated, channels with similar occupancy levels appear together in blocks of certain size, i.e., the DC is clustered in the frequency domain. This behavior was also observed in the rest of bands. To statistically characterize this aspect, the number of contiguous channels in each cluster (i.e., belonging to the same DC archetype) was evaluated for each measured spectrum band. The probability distributions of the resulting cluster sizes were evaluated and compared to several discrete models, from which it was observed that the geometric distribution [9] is able to provide reasonably accurate fits. Figure 5 shows some examples of empirical distributions of the number of channels per cluster and their corresponding geometric fits. Since the number of clusters within each band is significantly low, the distribution fitting does not provide highly reliable results but clearly indicates that the geometric distribution provides reasonably accurate fits. In order to facilitate the application of this model, Table 2 provides some reference values for the parameter p of the geometric distribution, extracted from empirical measurement data as the inverse of the average number of channels per cluster. The value of the parameter p can also be set following alternative methods. For example, if a particular average number of channels per cluster, M, needs to be reproduced, then it can be configured as $p = 1/M$. Moreover, it was empirically observed that the relation $p \approx C \cdot 10^{-3}$ holds for many of the analyzed spectrum bands, which can also be used to select the value of the geometric distribution parameter as long as the resulting value satisfies $p \leq 1$. Another option

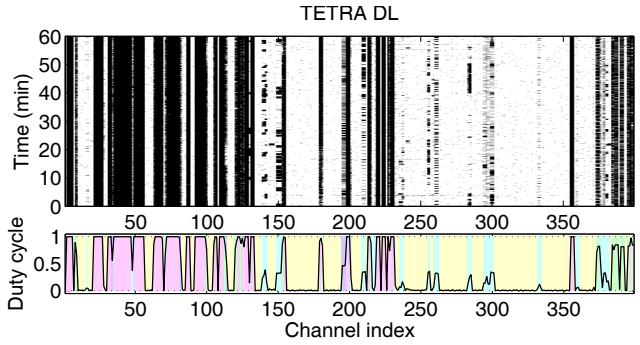

Figure 4: Empirical spectrum data for TETRA DL.

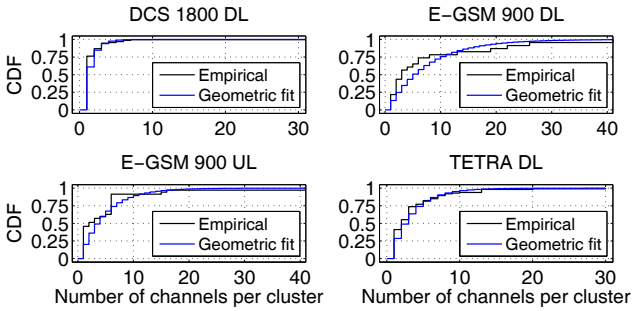

Figure 5: Empirical cluster size distributions.

would be to randomly generate the value of p from a uniform distribution within the interval $[0.1, 0.6]$ (see Table 2).

6. PROPOSED SIMULATION METHOD

The statistical models developed in previous sections can readily be employed and applied in analytical studies involving the time-frequency dimensions of spectrum usage. However, the proposed models can also be used and implemented in simulation tools for the design and dimensioning of secondary DSA/CR networks as well as the performance evaluation of DSA/CR techniques. To illustrate the applicability of such models in the context of simulation tools, a procedure to generate artificial spectrum data is described below. The proposed method is composed of three phases.

Phase 1: Generation of DC values.

- Step 1.1: Specify the number C of channels within the considered spectrum band.
- Step 1.2: Select a DC distribution function (beta or Kumaraswamy) and select appropriate values for the distribution parameters. The values provided in Table 1 can be used as a reference.
- Step 1.3: Based on the probability distribution resulting from Step 1.2, generate a set of C independent random numbers, which will constitute the set $\widehat{\mathbf{\Psi}} = \{\widehat{\Psi}_1, \widehat{\Psi}_2, \ldots, \widehat{\Psi}_c, \ldots, \widehat{\Psi}_C\}$ of DC values to be assigned to the C channels of the considered band.

Phase 2: Assignment of DC values to channels.

- Step 2.1: Define a set $\mathcal{A} = \{A_1, A_2, \ldots, A_n, \ldots, A_N\}$ of N DC archetypes along with the corresponding set $\mathbf{\Lambda} = \{\Lambda_0, \Lambda_1, \ldots, \Lambda_n, \ldots, \Lambda_N\}$ of $N+1$ DC thresholds, where $\Lambda_0 = 0$ and $\Lambda_N = 1$. A DC $\widehat{\Psi}_c$ belongs to archetype A_n if $\Lambda_{n-1} < \widehat{\Psi}_c \leq \Lambda_n$.
- Step 2.2: Based on the probability distribution resulting from Step 1.2, compute the elements of the set $\mathbf{\Pi} = \{\Pi_1, \Pi_2, \ldots, \Pi_n, \ldots, \Pi_N\}$, where $\Pi_n = P(A_n) = P(\Lambda_{n-1} < \widehat{\Psi}_c \leq \Lambda_n)$ represents the probability that a channel belongs to archetype A_n.
- Step 2.3: Classify the values of set $\widehat{\mathbf{\Psi}}$ into the archetypes of set $\mathcal{A}$ based on the threshold set $\mathbf{\Lambda}$. This will produce N subsets $\{\widehat{\mathbf{\Psi}}_n\}_{n=1,\ldots,N}$, one per DC archetype, satisfying $\bigcup_{n=1}^{N} \widehat{\mathbf{\Psi}}_n = \widehat{\mathbf{\Psi}}$ and $\bigcap_{n=1}^{N} \widehat{\mathbf{\Psi}}_n = \emptyset$.

Table 2: Fitted values for cluster size distributions.

Measured band	Parameter p	Measured band	Parameter p
Amateur	0.5625	Paging	0.3491
TETRA UL	0.0752	DCS 1800 UL	0.3824
TETRA DL	0.2857	DCS 1800 DL	0.6096
GSM 900 UL	0.2011	DECT	0.2000
GSM 900 DL	0.1322	ISM	0.3846

- Step 2.4: Select an appropriate value for the parameter p of the geometric distribution of the number of channels per cluster. The values provided in Table 2 or the alternative methods of Section 5.2 can be used.
- Step 2.5: Set to zero the elements of $\mathbf{\Psi} = \{\Psi_1, \Psi_2, \ldots, \Psi_c, \ldots, \Psi_C\}$, where Ψ_c represents the DC value finally assigned to channel υ_c. Set to zero the elements of the set $\boldsymbol{\alpha} = \{\alpha_1, \alpha_2, \ldots, \alpha_n, \ldots, \alpha_N\}$, where α_n represents a counter of the number of channels belonging to DC archetype A_n with an assigned final DC value. Define the counter $\alpha_C = \sum_{n=1}^{N} \alpha_n$ for the overall number of channels with an already assigned DC value. Repeat the following points until $\alpha_n = \eta_n$ for all n (i.e., $\alpha_C = \sum_{n=1}^{N} \eta_n = C$):
  1. Decide the DC archetype $A' = A_n$ for the next cluster (i.e., the next group of channels) by generating a uniformly distributed $U(0,1)$ random variate and comparing against the probabilities of set $\mathbf{\Pi}$.
  2. If this is not the first iteration of the process and the archetype A' resulting from point 1 is of the same type as the archetype A'' of the previously generated cluster, or if the number of channels for archetype $A' = A_n$ has already been reached ($\alpha_n = \eta_n$), go back to point 1 and recompute A' until the conditions $A' \neq A''$ and $\alpha_n < \eta_n$ are met. The condition $A' \neq A''$ is not necessary when there is a single DC archetype for which $\alpha_n < \eta_n$.
  3. Decide the number χ of channels that belong to the new cluster of type $A' = A_n$ as a random number drawn from the geometric distribution obtained in Step 2.4. If $\alpha_n + \chi > \eta_n$, then perform the correction $\chi = \eta_n - \alpha_n$ in order to meet the total number of channels per archetype.
  4. Select randomly χ DC values from subset $\widehat{\mathbf{\Psi}}_n$ (archetype A_n) that have not been assigned yet and form the subset $\widetilde{\mathbf{\Psi}} = \{\widetilde{\Psi}_1, \widetilde{\Psi}_2, \ldots, \widetilde{\Psi}_\chi\} \subseteq \widehat{\mathbf{\Psi}}_n$. Append subset $\widetilde{\mathbf{\Psi}}$ to the set of DC values already assigned, i.e., $\{\Psi_{\alpha_C+1}, \Psi_{\alpha_C+2}, \ldots, \Psi_{\alpha_C+\chi}\} = \{\widetilde{\Psi}_1, \widetilde{\Psi}_2, \ldots, \widetilde{\Psi}_\chi\} = \widetilde{\mathbf{\Psi}}$.

5. Update counters $\alpha_n = \alpha_n + \chi$ and $\alpha_C = \alpha_C + \chi$. Go to point 1.

Phase 3: Generation of time-domain occupancy sequences.

- Step 3.1: Select appropriate distributions $F_0(T_0)$ and $F_1(T_1)$ for the lengths T_0 and T_1 of idle and busy periods, respectively (e.g., generalized Pareto [6]).

- Step 3.2: Configure the parameters of the distributions selected in Step 3.1 in such a way that the channels' average DCs meet the DC values obtained in Step 2.5, i.e., $\mathbb{E}\{T_1^c\}/(\mathbb{E}\{T_0^c\} + \mathbb{E}\{T_1^c\}) = \Psi_c$, where $\mathbb{E}\{T_0^c\}$ and $\mathbb{E}\{T_1^c\}$ are the mean length of idle and busy periods, respectively, for the c-th channel, υ_c.

- Step 3.3: Generate for every channel a sequence of consecutive idle/busy periods whose lengths are drawn from the properly configured distributions $F_0(T_0)$ and $F_1(T_1)$. The sequences generated for every channel must be independent from each other. It is worth noting that the more sophisticated simulation method proposed in [6] can be used here in order to reproduce not only the distributions $F_0(T_0)$ and $F_1(T_1)$ but also the correlation properties of spectrum usage observed in real radio communications systems.

As it can be inferred from the proposed method, the steps conducted in the first phase guarantee that the DC values of the band follow an appropriate beta or Kumaraswamy distribution and consequently reproduce the corresponding average band DC. The second phase ensures that the DCs of contiguous channels respect the clustering properties observed in empirical measurements. Finally, the third phase provides the lengths of busy and idle periods for each channel so that not only the desired period length distributions are reproduced but also the appropriate DC distribution over frequency channels (and additionally the time-correlation properties of spectrum usage if the method proposed in [6] is employed).

In order to illustrate the proposed method, artificial spectrum data were generated for the TETRA DL band. The number of channels C was set accordingly and the parameters for the beta and geometric distributions were configured as shown in Tables 1 and 2. It is worth noting that these values correspond to the empirical measurements depicted in Figure 4. The DC archetypes considered in Section 5.2 were also employed in this case. The sequences of busy and idle periods were generated for a time period of 60 minutes using the method described in [6] in order to reproduce time-correlation properties. The obtained spectrum data are shown in Figure 6. The visual inspection and comparison with Figure 4 suggests that the proposed method is able to reproduce the statistical properties of spectrum in the time and frequency domains. To rigorously verify this statement, the artificial spectrum data were analyzed in the same manner as the field measurement data. The obtained results, not shown here due to the lack of space, indicated that the generated spectrum data had the same statistical properties as the empirical data in terms of the average band DC, the probability distribution for the channel DCs, the DC clustering distributions, the probability distribution for busy and idle period lengths and the time-correlation properties. This highlights the capability of the proposed models and simulation method to accurately capture and reproduce the statistical properties of spectrum usage observed for real systems in the time and frequency domains.

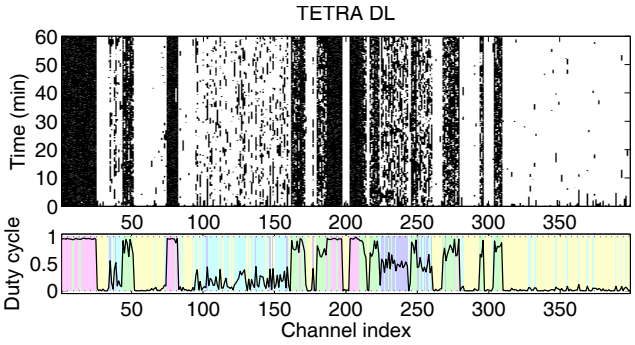

Figure 6: Artificial spectrum data for TETRA DL.

7. CONCLUSIONS

This paper has addressed the problem of jointly modeling spectrum occupancy in the time and frequency domains. The analysis of extensive empirical measurement results has revealed three important aspects to be taken into account for a realistic and accurate modeling of spectrum usage. First, the binary time-occupancy patterns of the channels within the same spectrum band are mutually independent. Second, the DC of the channels within the band follow beta or Kumaraswamy distributions. Third, the DC is clustered over frequency and the number of channels per cluster follows a geometric distribution. Based on these findings, a sophisticated procedure to generate artificial spectrum occupancy data for simulation and other purposes has been developed.

8. ACKNOWLEDGMENTS

This work was supported by the European Commission in the framework of the FP7 FARAMIR Project (Ref. ICT-248351) and the Spanish Research Council under research project ARCO (Ref. TEC2010-15198). The support from the Spanish Ministry of Science and Innovation (MICINN) under FPU grant AP2006-848 is hereby acknowledged.

9. REFERENCES

[1] I. F. Akyildiz, W.-Y. Lee, M. C. Vuran, and S. Mohanty. NeXt generation/dynamic spectrum access/cognitive radio wireless networks: a survey. *Comp. Networks*, 50(13):2127–2159, 2006.

[2] M. C. Jones. Kumaraswamy's distribution: A beta-type distribution with some tractability advantages. *Statistical Methodology*, 6(1):70–81, Jan. 2009.

[3] P. Kumaraswamy. A generalized probability density function for double-bounded random processes. *Journal of Hydrology*, 46(1-2):79–88, Mar. 1980.

[4] M. López-Benítez and F. Casadevall. Methodological aspects of spectrum occupancy evaluation in the context of cognitive radio. *European Trans. on Telecomms.*, 21(8):680–693, 2010.

[5] M. López-Benítez and F. Casadevall. Discrete-time spectrum occupancy model based on markov chain and duty cycle models. In *Proc. IEEE 5th Int'l. Symp. on Dynamic Spectrum Access Networks (DySPAN 2011)*, pages 1–10, May 2011.

[6] M. López-Benítez and F. Casadevall. Modeling and simulation of time-correlation properties of spectrum use in cognitive radio. In *Proc. 6th Int'l. ICST Conf. on Cognitive Radio Oriented Wireless Networks (CrownCom 2011)*, June 2011.

[7] M. López-Benítez and F. Casadevall. A radio spectrum measurement platform for spectrum surveying in cognitive radio. In *Proc. 7th Int'l. ICST Conf. on Testbeds and Research Infrastructures for the Development of Networks and Communities (TridentCom 2011)*, pages 1–16, Apr. 2011.

[8] M. A. McHenry et al. Spectrum occupancy measurements. Technical report, Shared Spectrum Company, 2004-2005.

[9] A. Papoulis and S. U. Pillai. *Probability, random variables, and stochastic processes*. McGraw-Hill, Boston, 4 edition, 2002.

[10] H. Urkowitz. Energy detection of unknown deterministic signals. *Proceedings of the IEEE*, 55(4):523–531, Apr. 1967.